

The use of impedance matching capillaries for reducing resonance in rosette infrasonic spatial filters

Michael A. H. Hedlin^{a)}

*Institute of Geophysics and Planetary Physics, Scripps Institution of Oceanography,
University of California, San Diego, La Jolla, California 92093-0225*

Benoit Alcoverro^{b)}

*Commissariat à l'Énergie Atomique, Département Analyse et Surveillance de l'Environnement, BP 12,
91680 Bruyères le Chatel, France*

(Received 19 May 2003; revised 2 March 2004; accepted 1 April 2004)

Rosette spatial filters are used at International Monitoring System infrasound array sites to reduce noise due to atmospheric turbulence. A rosette filter consists of several clusters, or rosettes, of low-impedance inlets. Acoustic energy entering each rosette of inlets is summed, acoustically, at a secondary summing manifold. Acoustic energy from the secondary manifolds are summed acoustically at a primary summing manifold before entering the microbarometer. Although rosette filters have been found to be effective at reducing infrasonic noise across a broad frequency band, resonance inside the filters reduces the effectiveness of the filters at high frequencies. This paper presents theoretical and observational evidence that the resonance inside these filters that is seen below 10 Hz is due to reflections occurring at impedance discontinuities at the primary and secondary summing manifolds. Resonance involving reflections at the inlets amplifies noise levels at frequencies above 10 Hz. This paper further reports results from theoretical and observational tests of impedance matching capillaries for removing the resonance problem. Almost total removal of resonant energy below 5 Hz was found by placing impedance matching capillaries adjacent to the secondary summing manifolds in the pipes leading to the primary summing manifold and the microbarometer. Theory and recorded data indicate that capillaries with resistance equal to the characteristic impedance of the pipe connecting the secondary and primary summing manifolds suppresses resonance but does not degrade the reception of acoustic signals. Capillaries at the inlets can be used to remove resonant energy at higher frequencies but are found to be less effective due to the high frequency of this energy outside the frequency band of interest. © 2005 Acoustical Society of America. [DOI: 10.1121/1.1760778]

PACS numbers: 43.28.Dm, 43.28.Ra, 43.50.Cb [LCS]

Pages: 1880–1888

I. INTRODUCTION

A. Infrasonic and global nuclear monitoring

The Comprehensive Nuclear Test-Ban Treaty (CTBT) was made available for signature at the United Nations in September of 1996. This has led to increased interest in monitoring globally for nuclear testing activity at all yields which in turn has led to the development of the four-network International Monitoring System (IMS). The IMS includes infrasound, radionuclide, seismic, and hydroacoustic stations. Although the primary goal of the system is to monitor Earth's atmosphere, solid interior, and oceans for nuclear testing activity, an additional benefit of the continuously monitoring system is that it will allow detection, tracking, and analysis of other man-made and natural phenomena on an unprecedented global scale.

This paper is concerned with the infrasound component of the IMS (Christie *et al.*, 2001). As of November 2001, 10 of the planned 60 microbarograph arrays were operating and another 10 were under construction. Completion of the entire network is expected to take several more years. Each infra-

sound array will comprise four to eight sensors with a baseline of 1 to 3 km. Sensors in the infrasound network are designed to detect signals between 0.01 and 8 Hz, but the array geometry is designed for optimal detection in the 0.1–1 Hz range. Infrasonic pressure data are collected at each site at 20 samples per second (sps) along with wind speed and direction sampled at 1 sps. The operating arrays transmit data to the International Data Center (IDC) in Vienna, Austria. One array (Fig. 1) is in the Anza-Borrego desert south of Palm Springs, CA.

B. Reduction of infrasonic noise

The principal source of noise in the frequency band of interest to the nuclear monitoring community is atmospheric turbulence. As a result, all pressure data are filtered in the field by a spatial wind-noise-reducing system (Daniels, 1959; Burrige, 1971; Grover, 1971). The filter averages out pressure variations that are due to local turbulence and increases the signal-to-noise ratio (SNR).

The infrasound monitoring network is designed to provide monitoring of the atmosphere at all points on the globe. As a result, the noise reducing systems are required to be omnidirectional. A recent design of a spatial filter by Alcov-

^{a)}Electronic mail: hedlin@ucsd.edu

^{b)}Electronic mail: benoit.alcoverro@cea.fr

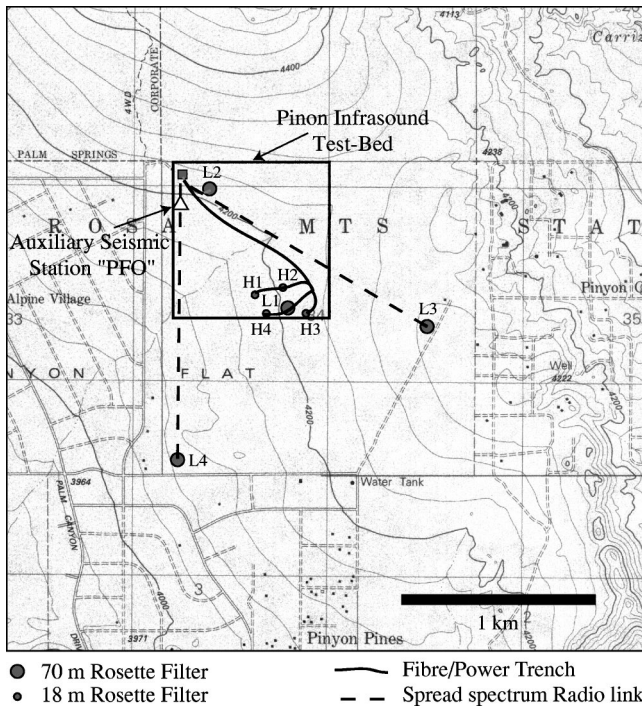


FIG. 1. The eight-element infrasound array at Pinon Flat, CA comprises four long-period elements (L1–L4) in a centered triangle spanning less than 2 km and four short-period elements (H1–H4) in an irregular quadrilateral near the center. The terrain slopes down gently to the southwest. The contour interval is 40 ft. (12.2 m).

erro (1998) consists of several clusters, or rosettes, of low-impedance inlets. Low-impedance inlets are preferred as they require essentially no maintenance. Each inlet in a cluster is connected to a “secondary” summing manifold by a solid pipe. A solid pipe connects each secondary summing manifold to one primary summing manifold or directly to the sensor. All pipes are solid, and thus all acoustic energy that propagates to the sensor enters the filter via the inlets. The signals are integrated acoustically at the summing manifolds. Christie (Provisional Technical Secretariat, Comprehensive Nuclear-Test-Ban Treaty Organization) has proposed several modifications to Alcoverro’s original rosette design (Christie, 1999). The Christie rosette filters range from 92 ports distributed over an area 18 m across to 144 ports spanning an area 70 m across (Fig. 2). The smaller filter is considered to be more effective at high frequencies at windy sites. The 70-m aperture filter is considered appropriate for windy sites that require suppression of noise between 0.02 and 0.7 Hz.

C. Resonance in rosette filters

As discussed by Hedlin *et al.* (2003) and Alcoverro and LePichon (2004), one drawback of the rosette filter design currently in use at IMS array sites is internal resonance. Impedance discontinuities exist at the inlets to the summing manifolds, the microbarometer, and the inlets. The resonance is predicted and observed above 3 Hz in data from the 18-m rosette systems (Fig. 3). Resonance peaks exist above 0.7 Hz and peaks at 2.65 and 7.95 Hz in data from the 70-m rosette systems (Fig. 3). Due to attenuation, the resonant energy is seen in data from the 70-m rosettes at all frequencies above 0.7 Hz. Higher overtones are believed to exist at higher fre-

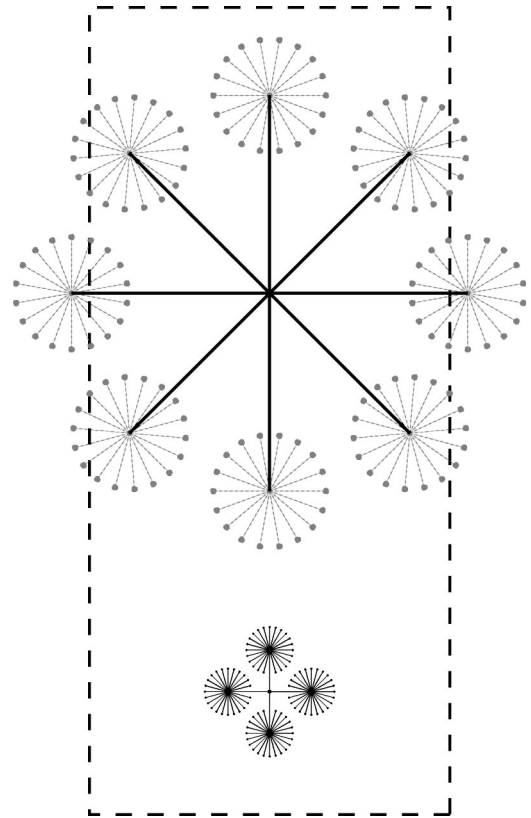


FIG. 2. Two rosette filters considered in this paper are shown to scale with a National Football League playing surface (dashed rectangle). The playing surface is 50 m wide by 112 m long. The 18-m filter comprises 92 low-impedance inlets in four rosettes. The 70-m filter comprises 144 inlets arranged in eight rosettes. In both filter designs, the inlets are connected by solid pipe to secondary summing manifolds at the center of each rosette. The secondary manifolds are connected to a primary manifold, which is connected by a short pipe to the sensor. Each inlet is located the same distance along solid pipe from the sensor. Signals arriving from directly above the filter are summed in phase. Adjacent ports in the 70-m filter are separated by 2.79 m. Adjacent ports in the 18-m filter are 0.85 m apart. For this study, we used the filters at locations L2 and H1 in the array IS57. The first experiment involved simplified rosette filters consisting of eight 27 m pipes attached to a primary summing manifold. These filters are shown to scale in this figure as the solid black lines. The inlets in some of the filters were fitted with capillaries.

quencies but are removed in our data by the anti-aliasing filter, which takes effect at 8 Hz. The resonance is observed at all wind speeds (Hedlin *et al.*, 2003; Alcoverro and LePichon, 2004). The resonance results in an increase in noise levels and the signal waveform may be significantly distorted.

D. Rationale for this study

There are two primary objectives for this study. The first is to identify the reflection points that give rise to resonant energy in the passband below 8 Hz in the 18- and 70-m rosette filters. Toward this end we present data collected by simplified rosette filters that comprise just eight inlets and span 54 m (Fig. 2). We use the theory of Alcoverro and LePichon (2004) to model the frequency response of the simplified and full rosette filters. The second, and key, objective of this paper is to investigate the use of impedance matching capillaries to suppress, or remove, resonance from these fil-

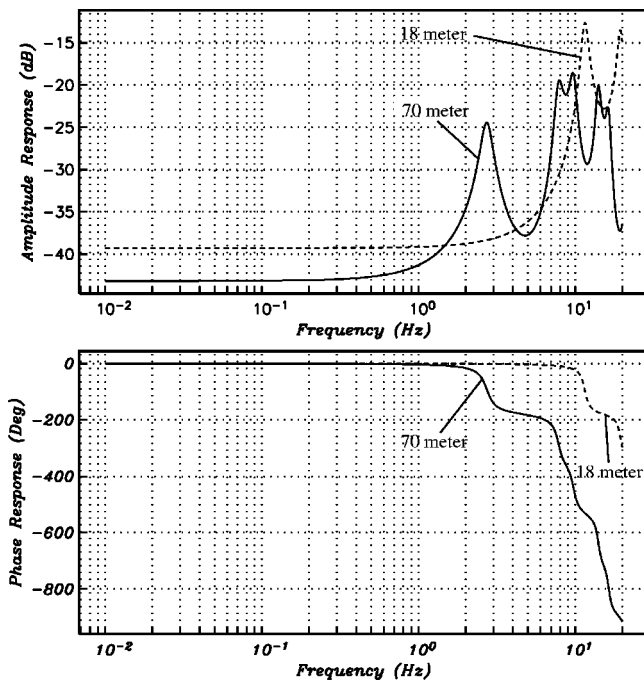


FIG. 3. Predicted amplitude and phase response of the 18-m/92-rosette filter (dashed curve) and the 70-m/144-rosette filter (solid curve) for one inlet. The resonance peaks coincide with significant change in the phase response of the filter. The long-period response is given by $-20 \log_{10}(N)$, where N is the number of inlets.

ters. We predict theoretically the response of simple and full rosette filters equipped with impedance matching capillaries and compare the theoretical results with recorded data. We use continuous recordings of atmospheric noise and a large acoustic signal to validate the theoretical results.

II. THE PINON FLAT INFRASOUND TEST-BED

All of our experiments have been conducted at the infrasound test-bed at the Pinon Flat Observatory in southern California. The observatory is described in detail by Hedlin *et al.* (2003) and so only a brief description is given here. The observatory is located in the desert south west of Palm Springs. This site has been useful for studies of infrasonic wind-noise reducing systems as wind speeds vary from near zero at night to above 15 m/s during the day. The observatory is sparsely vegetated with Pinon pine trees and there is essentially no ground cover. The IMS infrasound array IS57 is located at the observatory (Fig. 1). The array comprises eight sensors on a baseline of 2 km and uses both the high-frequency, 18-m, and low-frequency, 70-m, rosette filters described earlier.

III. EXPERIMENTAL LAYOUT

A typical experimental layout is as described by Hedlin *et al.* (2003). Each site includes an MB2000 aneroid microbarometer. The pressure data are low-pass filtered below 8 Hz and sampled at 20 sps by a Reftek digitizing system. Air temperature and wind velocity were collected at 1 sps at heights of 1 and 2 m, respectively. Data from the temporary sites were transmitted in real-time to our laboratory in La Jolla via a 2.2-GHz spread-spectrum radio link. All recording

devices were housed in insulating cases to shield them from the extreme desert conditions. In all experiments, one microbarograph sensor was attached to a single, low-impedance, inlet located 5 cm above the ground and was used to indicate the level of background noise. All other sensors were attached to a noise-reducing system. With the exception of two sites, all systems were deployed temporarily. Two of the sites used for this study are in the IMS infrasound array IS57. Data from the array sites were transmitted to our laboratory via phone lines.

IV. PRELIMINARY TESTS OF CAPILLARIES

A. Observed and predicted resonance

The infrasonic noise-reducing filter developed by Daniels in the late 1940s comprised a single pipe with inlets distributed along its length (Daniels, 1959). The prototype was 603 m long with 100 inlets. The pipe diameter, and thus its characteristic impedance, changed, in steps, at each of the inlets, the section increasing toward the sensor. The acoustic impedance of each inlet was selected in the aim that the parallel combination of the inlet and the characteristic impedance of the small pipe was equal to the characteristic impedance of the larger pipe at the location of the inlet. Acoustic energy propagating in the pipe away from the sensor would not reflect back to the sensor, but impedance and time lag at each inlet are different.

As shown in Fig. 2, a rosette filter consists of inlets connected via solid pipes and summing manifolds to a microbarograph located at the center. In the 70-m rosette filters in use at the IMS array IS57, the pipes connecting the central, primary, summing manifold with the secondary summing manifolds are 27 m long, with an internal diameter of 2.1 cm. The characteristic acoustic impedance of these pipes is 1.202 mega-ohms ($M\Omega$), where acoustic resistance is calculated using SI units (i.e., Ns/m^5). The secondary summing manifolds are connected via 8-m-long pipes to the inlets. These pipes have an inner diameter of 1.6 cm and a characteristic impedance of 2.07 $M\Omega$. As discussed by Hedlin *et al.* (2003), resonance peaks are observed at 2.65 and 7.95 Hz. Resonance modeling reproduces these resonance peaks (Fig. 3) and indicates that the reflections that give rise to these peaks occur at the secondary and primary summing manifolds. Data from the 18-m rosette filters do not exhibit a prominent spectral peak due to resonance, but a gradual increase in energy with increasing frequency above 2 Hz. Peaks above the Nyquist frequency at 10 Hz are predicted (Fig. 3).

To verify that the reflections that produce significant resonance peaks below 10 Hz are caused by reflections at the summing manifolds, and not at the inlets, and that capillaries can remove the resonant energy without also attenuating the signals of interest, we conducted a field experiment with simple, eight-arm, filters. As shown in Fig. 2, we constructed filters that spanned 54 m, or exactly the area inside the secondary summing manifolds in a 70-m rosette filter. A simple, eight-arm, filter is depicted in Fig. 2 as the solid black lines.

The experiment with simple filters occurred from 1 November, 2001 to 14 January, 2002. For this experiment, we

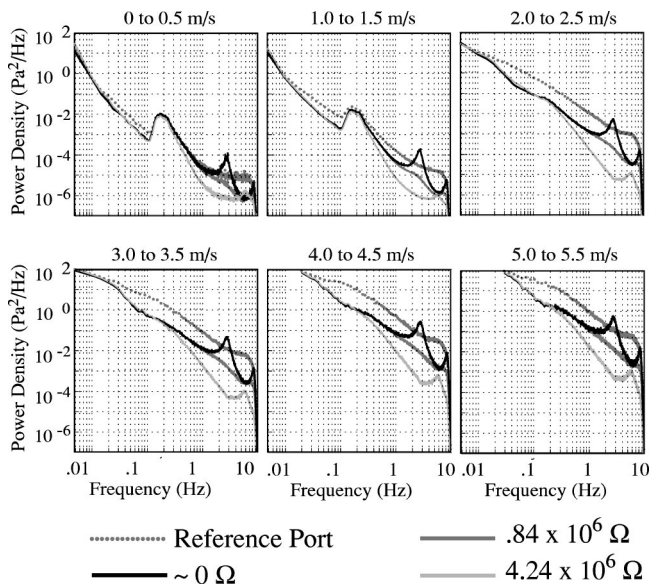


FIG. 4. Robust estimates of the dependence of infrasonic noise on wind speed and frequency can be obtained by stacking spectral estimates taken at different times but during similar wind conditions. To accomplish this, we associate each spectral estimate with a single wind-speed value: the average wind speed from the 15-m interval spanned by the spectrum. We stack spectral estimates after binning them by wind speed into bins that span 0.5 m/s starting at 0.0 m/s. The six panels in this figure show binned and stacked spectra taken at the reference port (dotted) and three eight-arm simple “rosette” filters. The filters were identical except for the acoustic resistances installed at the inlets. The black curves represent data from the filter with no acoustic resistance installed at the inlets. The dark gray and light gray curves represent data from filters with intermediate and high acoustic impedance capillaries installed at the inlets.

co-located three simple filters with a reference site. The simple filters used in this test were identical, except at the inlets. One filter (black curves in Fig. 4) was equipped with low-impedance inlets. The other two filters were equipped with capillaries at each of the inlets. One filter (dark gray curves) included acoustic resistances at the inlets of 0.84 MΩ. The other (light gray curves) was equipped with higher acoustic resistance at the inlets of 4.24 MΩ. These resistances were selected to bracket the characteristic impedance of the 27-m pipes connecting the inlets with the primary summing manifold and the microbarograph at each site.

Spectra from the four sites are displayed in Fig. 4. In this figure, we show binned and stacked spectral density from the four sites at wind speeds ranging from 0–0.5 m/s to 5.0–5.5 m/s. In each panel, the dotted curves represent ambient noise levels recorded at the reference site. The growth of infrasonic noise levels with increasing wind speed is evident. As shown in Fig. 4, the system with open inlets produces a substantial resonance peak in the data at 2.65 Hz at all wind speeds. The first resonance peak in data from the full 70-m rosette filters was also observed at 2.65 Hz (Hedlin *et al.*, 2003). This provides empirical evidence of the finding made by Hedlin *et al.* (2003) that the reflections that give rise to the resonance at this frequency are occurring at the secondary summing manifolds, and not at the inlets. The lowest resonant frequency is determined by the propagation time in the longer (27 m) pipe in the noise filter.

As shown in Fig. 4, it is possible to blunt, or entirely remove, the resonance peak at 2.65 Hz by adding acoustic

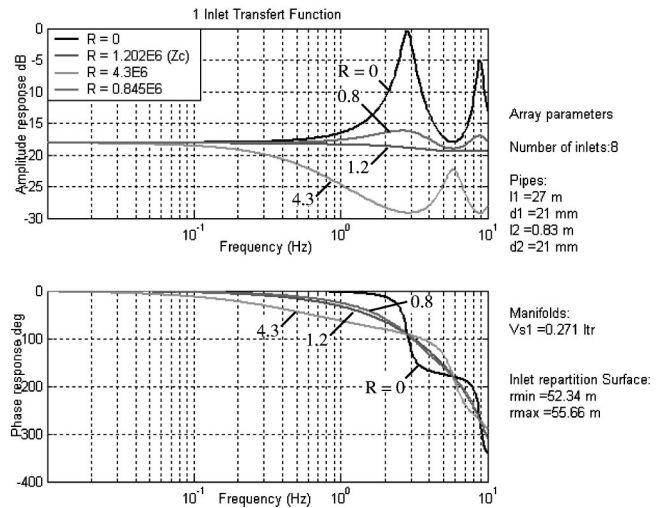


FIG. 5. Theoretical predictions of amplitude and phase response for the eight-arm “rosette” filter systems. The theoretical predictions match closely the spectra obtained from recorded data.

resistance at the inlets. The system with inlet resistance that is less than the characteristic impedance of the pipe shows some evidence of resonance. The system with the high inlet resistance shows a marked decrease in noise levels at 0.3 Hz with no resonance peak at 2.65 Hz. A resonance peak is observed at 5.3 Hz, or exactly double the frequency of the unmodified system. The spectral results indicate that resonance can be controlled by adding acoustic resistance at the inlets, but suggests that high resistance will attenuate the energy across a broad band.

The response of the eight-arm “simple” filters has been calculated using the method of Alcoverro and Le Pichon (2004). Four simple filters were considered. The first three were exactly as tested in the field. The fourth filter included acoustic resistance at the inlets of 1.202 MΩ, equal to the characteristic impedance of the 27-m pipes leading to the primary summing manifold. The capillaries are modeled as a pure resistance with a value depending on the diameter and the length of the small pipe used. These elements are inserted in the electro-acoustic scheme described by Alcoverro and Le Pichon (2004) between manifold and pipe or between the radiating impedance and the pipes at the input of the circuit. The capillaries could be inserted elsewhere inside the model if required. The frequency response is calculated from this modified electro-acoustic scheme by a matrix method. Using this method, noise reduction could also be simulated but is not presented here. These results are summarized in Fig. 5. The simulations correctly predict both the position of the resonance peaks and the amplitude for each of the systems tested in the field. The system with no acoustic resistance at the inlets is predicted to yield resonance at 2.65 Hz, 15 dB above the system with intermediate resistance. The system with 4.24 MΩ capillaries shows an 11-dB attenuation near 3 Hz. This is exactly what was observed in the recorded data (Fig. 4). The anti-aliasing filter applied to the recorded data complicates comparison of the higher frequency resonance peak at 7.95 Hz. Only the synthetics calculated for the system with capillaries at the inlets with acoustic resistance

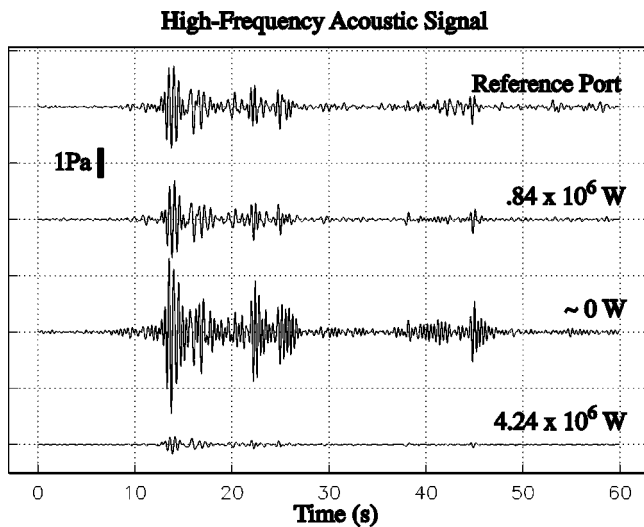


FIG. 6. An acoustic signal recorded by the reference site and the eight-arm filters. As expected, the system with the high acoustic impedance capillaries at the inlets overattenuates both the noise and the signal. The system with no acoustic resistance at the inlets (second trace from the bottom) produces highly resonant recordings. Only the system with the intermediate acoustic resistance capillaries ($0.84 \text{ M}\Omega$) installed at the inlets provided a recording that closely resembles the one provided by the reference site.

equal to the characteristic resistance of the pipes leading to the primary summing manifold are predicted to have no resonance peaks.

B. Analysis of a signal

On 21 November, 2001, a large signal was recorded by all systems in this experiment. Analysis of IS57 array data places the source at an azimuth of 240° . The phase velocity of the energy was 330 m/s . Although the cause of this signal remains unknown, the signal was coherent across the IS57 array and the simple spatial filters considered in this experiment, and provides an opportunity to examine the effect of capillaries on incident signals. As shown in Fig. 6, the incident wavetrain spans $\sim 40 \text{ s}$. The recordings of the signal via the reference site, and via the simple filter equipped with low impedance inlets, are similar, however the data from the filter exhibits a substantial coda. The signals recorded by the reference system are more impulsive. The system with intermediate acoustic resistances ($1.202 \text{ M}\Omega$) installed at the inlets produced a recording of the event that matches, much more closely, the character of the reference recording. The system with high resistance capillaries ($4.3 \text{ M}\Omega$) installed at the inlets produced a heavily attenuated copy of the signal. As predicted by the theory, the resistance above the characteristic impedance of the pipe overattenuates signal and noise at frequencies above 0.1 Hz by 11 dB . The high-impedance capillaries are predicted to low-pass filter the data below 0.2 Hz . The high inlet resistance that has proved able to remove much of the resonance has had an obvious, negative, effect on the incident signal.

V. TESTS OF CAPILLARIES ON ROSETTE FILTERS

The theory of Alcoverro and LePichon (2004) has been used successfully to estimate the effect of acoustic resistance

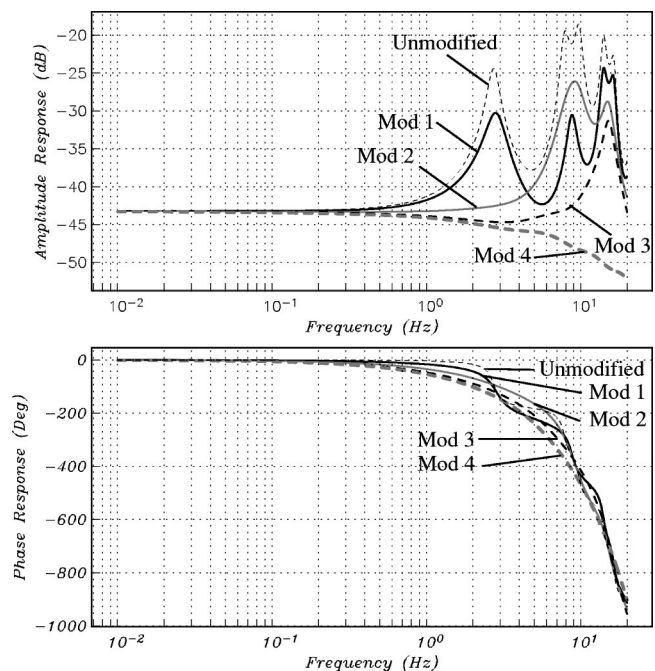


FIG. 7. Simulations of the original and modified 70-m aperture rosette filter frequency responses are shown in this figure. The systems with capillaries at the inlets (modification 1), at secondary summing manifolds in the pipes leading to the primary summing manifold (modification 2), at both the inlets and the secondary summing manifolds (modification 3), at the inlets and both summing manifolds (modification 4) are represented by the heavy black, heavy gray, heavy dashed black, and heavy dashed gray curves, respectively. The unmodified system is represented by the light dashed curves.

at the inlets of simplified rosette filters on resonance. The theory has further indicated that adding acoustic resistance at the inlet equal to the characteristic impedance of the 27-m -long pipe will remove all evidence of resonance near 2.65 Hz . Having validated the theory on simple filters, we now turn to full rosette filters.

A. Predictions of noise reduction in 70-m rosettes

We begin with the 70-m rosette filters in use at the IS57 infrasound array and shown in detail in Fig. 2. As shown in Fig. 7 (heavy solid black curve; modification 1), adding $2.07 \text{ M}\Omega$ acoustic resistance at the inlets, equal to the characteristic impedance of the 8-m pipe connecting the inlets with the secondary summing manifolds, reduces the resonance peak corresponding to the first fundamental frequency inside the 8-m pipes, near the Nyquist frequency. As shown by the heavy solid gray curve in the same figure, installing $1.202 \text{ M}\Omega$ acoustic resistance (capillaries 0.051 and 0.024 m in diameter) at each secondary summing inside the 27-m pipes leading to the primary summing manifold (modification 2) removes the main resonance peak near 2.65 Hz and its odd overtone near 7.95 Hz . The resistance at the secondary summing manifolds removes the fundamental resonance peak at 2.65 Hz and the first, odd, overtone near the Nyquist, but leaves the fundamental resonance occurring in the shorter pipes in the rosette clusters. The 180° phase shift that occurs at 2.65 Hz in the open system is blurred across a broader frequency band in the system that includes capillaries at the secondary summing manifolds.

It is possible to attack both the resonance occurring in

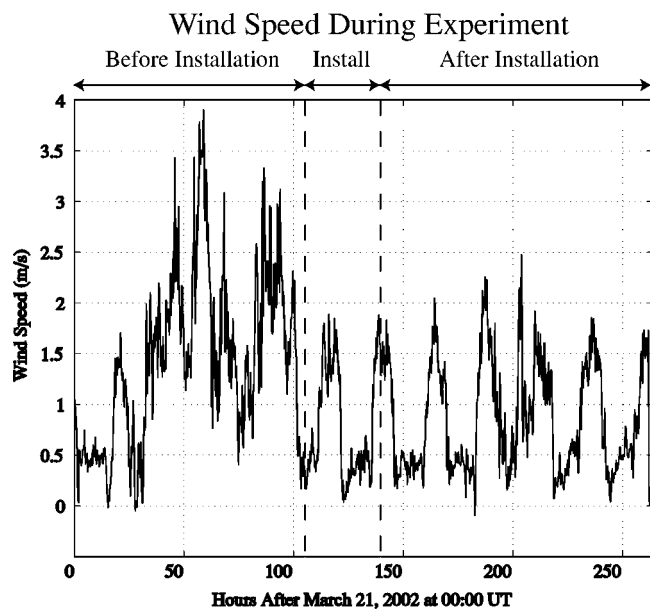


FIG. 8. Wind speeds during the experiment with the 70-m rosette filters.

the 27-m pipes, and the resonance in the 8-m pipes, by adding capillaries at the secondary summing manifolds and at the inlets (modification 3). A simulation of this is represented by the heavy dashed black curve in Fig. 7. Resonance energy above 5.0 Hz can be largely removed by modifying the filter in this manner. The resonance peak observed above 10 Hz (the heavy dashed black curve in Fig. 7) is due to resonance in the pipe that connects the primary summing manifold to the sensor. This can be removed by installing another 2.07 M Ω capillary adjacent to the primary summing manifold in that pipe. Synthesis of this modification (the fourth) is represented by the heavy dashed gray curves in Fig. 7.

As pointed out by Hedlin *et al.* (2003), the additional labor of installing capillaries at the 144 inlets and in the pipe between the primary summing manifold and the sensor is unlikely to be beneficial as the plane wave response of the filter to nonvertically incident signals severely attenuates energy above 3–4 Hz. The response of the system with capillaries at the primary and secondary summing manifolds as well as at the inlets is also not flat above 1 Hz. For these reasons, we proceeded with a test of capillaries at the secondary summing manifolds only.

B. Experiments with 70-m filters

To test the theoretical predictions, we installed 1.202 M Ω capillaries adjacent to the secondary summing manifolds in the main pipes leading to the primary summing manifold at the “L2” site in the array IS57. The other three 70-m filters (L1, L3, and L4 identified in Fig. 1) were left unchanged to provide a reference. We also collected pressure data with a microbarometer attached to a single inlet. The wind speed during this experiment before, during and after the modifications at L2 is shown in Fig. 8. The experiment spanned 11 days in March 2002. Diurnal variations in the wind speed are seen throughout the experiment with wind

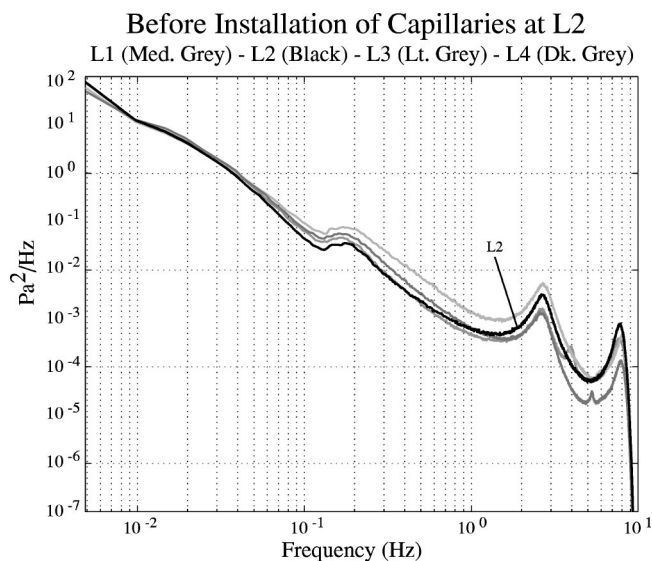


FIG. 9. Spectral density estimates taken from data collected at four 70-m rosette filters before any were modified. All spectra show significant resonance peaks at 2.65 and 7.95 Hz.

speeds varying from near zero to above 3.5 m/s. The wind speeds before the modification of L2 were slightly higher than those recorded after the change.

Stacked power spectral estimates from all 70-m filters prior to the installation of the capillaries at site L2 are shown in Fig. 9. The resonance peaks are evident in the data from all sites. In Fig. 10 we show a photograph of one capillary and a diagram showing its location in relation to the secondary summing manifold. The installation of each capillary required one person \sim 2 h. In Fig. 11, we show power spectral estimates taken from data collected after all eight capillaries were installed in the L2 filter. The results are striking. Very significant resonance peaks are observed in the data from the unmodified filters. No evidence of resonance in the data from the modified filter is seen below 5.0 Hz. The only sign of resonance, as predicted by the calculations shown in Fig. 7, is seen between 5 and 8 Hz. This is beyond the optimal pass-band of the 70-m rosette filters (Hedlin *et al.*, 2003).

C. Theory and experiment with 18-m rosette filters

As predicted in Fig. 3, resonance is expected to become apparent in data collected via the 18-m rosette filter at \sim 2.0 Hz. It is expected to rise to \sim 15 dB above background by 10 Hz. The problem with resonance in the 18-m rosette filters is less significant than it is in the large-aperture rosette filter considered in the previous section. As shown in Fig. 12, simulations of 18-m rosette filter frequency response equipped with impedance matching capillaries at both the secondary summing manifolds and at the inlets indicate that these can further improve the amplitude response of the filter. However, the phase shift is predicted to deviate from zero at frequencies below 1 Hz. In Fig. 12, we show the predicted amplitude and phase response of three 18-m rosette filters. The unmodified filter response is given by the dashed curve. The first resonance peak is centered just above 11 Hz and is due to resonance between the summing manifolds. A 180 $^\circ$ phase shift occurs at that frequency. A second reso-

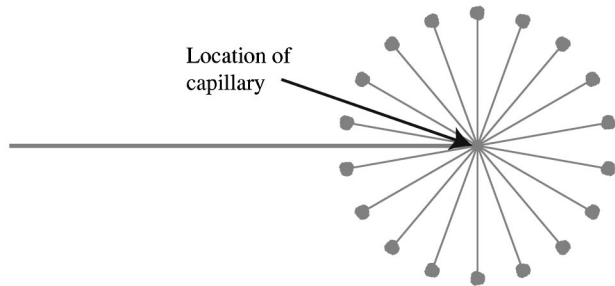
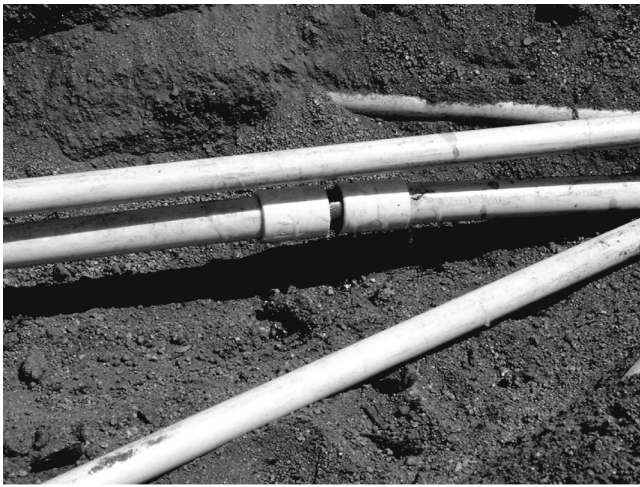


FIG. 10. A photograph of a capillary plug installed in a pipe connecting the primary and secondary summing manifolds. The capillary was installed 30 cm from the secondary summing manifold as shown in the lower diagram. The other pipes shown in the photograph connect the secondary summing manifold with inlets.

nance peak is observed near 19 Hz and is due to resonance in the inlet clusters between the inlets and the secondary summing manifolds. Installing 2.07 M Ω capillaries at the inlets removes the higher frequency resonance peak but leaves most of the resonant energy below the Nyquist frequency at 10 Hz. Installing 2.07 M Ω capillaries adjacent to the second-

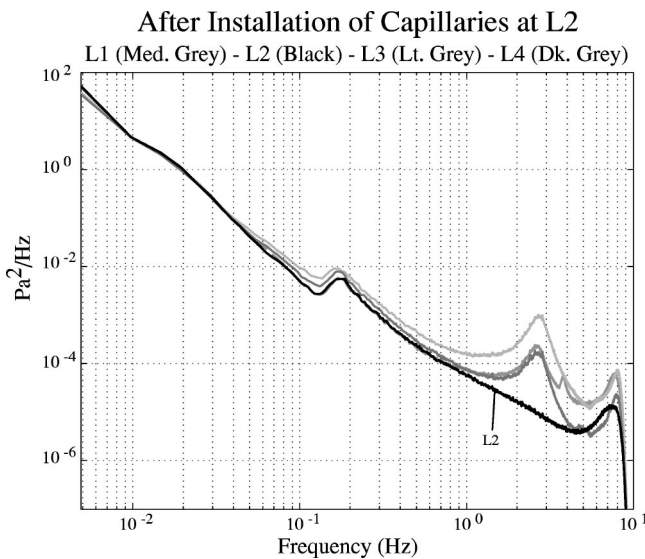


FIG. 11. Spectral density estimates taken from data collected after the capillary plugs were installed at site "L2" (black curve). The capillaries have removed the resonance peak at 2.65 Hz.

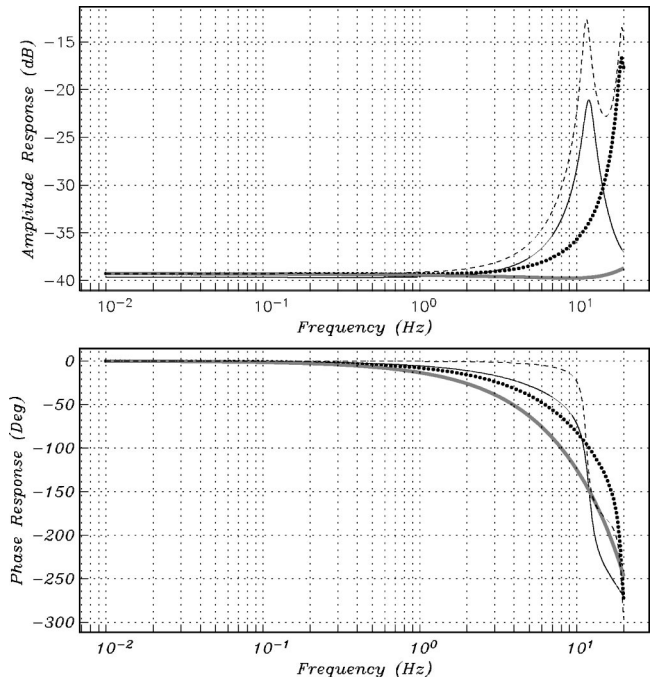


FIG. 12. Theoretical predictions of amplitude and phase response for the 18-m filter with and without capillaries. The unmodified filter is represented by the dashed curves. The filter with capillaries at the inlets, at the secondary summing manifolds, and at both locations are represented by the solid black, dotted black, and solid gray curves.

ary summing manifolds in the pipes leading to the primary summing manifold effectively removes the resonance between the summing manifolds. The amplitude response is improved by 13 dB at 10 Hz (dotted black curve in Fig. 12). When the system is equipped with capillaries at both inlets and secondary manifolds, the frequency response is flat up to 20 Hz (gray curve in Fig. 12). In Fig. 13, we show stacked spectra taken from all four 18-m rosette filters at the IS57 array before any were modified. The unmodified 18-m filters are inferior to the modified long-period 70-m filter at all frequencies. As shown by Hedlin *et al.* (2003) and by Alcoverro and LePichon (2004), unmodified 70-m filters outperform the 18-m filters only at frequencies below ~ 1.0 Hz.

Figure 14 shows spectral density estimates from the reference site and from an 18-m rosette filter before and after the capillaries were installed at the secondary summing manifolds. The capillaries remove the resonance above 1 Hz. The overall decrease of noise levels at all frequencies above 0.05 Hz is due to atmospheric conditions and is not due to the capillaries. Data from the unmodified 18-m filters showed the same decrease in energy.

VI. CONCLUDING REMARKS

Our research indicates that the reflections that produce resonance below 10 Hz in the 18- and 70-m rosette filters occur at the summing manifolds connected to the end of the longer pipe. Reflections that occur at the inlets artificially inflate spectral amplitudes at frequencies above 5 Hz. We find the theoretical method of Alcoverro and LePichon (2004) accurately predicts the frequency response of rosette

After Installation of Capillaries at L2

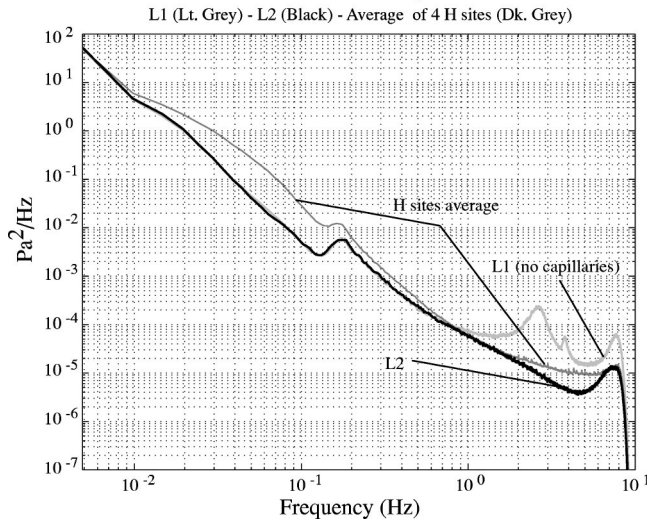


FIG. 13. Spectral density estimates from sites L1, L2 (both 70-m rosettes) and the 18-m rosettes. The data were taken after the L2 filter (black curve) was modified with the capillaries but before any modifications were made to the 18-m filters. The modified L2 70-m filter outperforms the unmodified 18-m filters at all frequencies. The resonance energy is first seen in the data from the 18-m rosette filters (the dark gray curve) at $\sim 1-2$ Hz. The peak observed in all spectra between 0.1 and 0.2 Hz is due to microbaroms (Donn and Posmentier, 1967).

filters. The method also accurately predicts the effect of capillaries installed at any point inside the filters.

We conclude that the greatest gain in performance of the rosette filters is produced by installing impedance matching capillaries adjacent to the secondary summing manifolds in the pipes leading to the primary summing manifold. Installation of capillaries at the inlets is physically demanding, due to the large number of inlets involved, and offers little if any benefit to sensitivity of the filters due to the plane-wave response of the filters. As shown by Hedlin *et al.* (2003), the

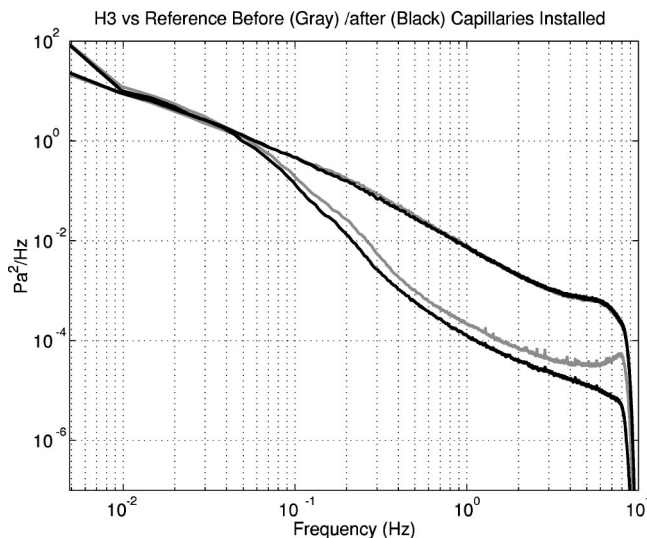


FIG. 14. Spectral density estimates from the reference site (upper curve) and from an 18-m rosette filter before (gray curve) and after (lower black curve) the capillaries were installed at the secondary summing manifolds. The capillaries have removed the resonance above 1 Hz. The observed decrease of noise levels at all frequencies above 0.05 Hz is not due to the capillaries but is due to atmospheric conditions.

plane wave response of the 70-m system is strongly dependent on frequency above 3 Hz. Above 5.0 Hz, much of the energy is attenuated. Adding capillaries at the inlets attacks resonant energy in a band that is already of limited value for the study of infrasonic signals.

There is an additional, practical, motive for not installing capillaries at the inlets but placing them in the interior of the filter. The capillary plugs installed in the 70- and 18-m rosette filters have an inner diameter of 2.4 mm. The desired acoustic resistance was achieved by varying the length of the capillary. Although the capillaries have been shown to provide an effective reduction of resonance inside the rosette filters, it will take long-term exposure to the elements to determine if the capillaries will, in practice, remain clear and remain effective without adverse side effects. If, with time, the capillaries become partially, or fully, occluded, the response of the overall rosette filter will be degraded. A fully occluded capillary will reduce the overall reduction of long-period noise provided by the filter by rendering useless an entire rosette of inlets. Partially occluded capillaries would have other adverse effects on the data as we have seen; the phase shift of the filter is determined, to some extent, by the capillary resistances. The rosette filters are not used alone, but as part of an array. It is essential that the amplitude and phase response of all filters in the array be matched. If changes in the acoustic resistance of the capillaries changes with time, and in a manner that differs between filters, the overall response of the array could be degraded. A bias could be introduced into the azimuths obtained from the array data.

Regardless of the location of the capillaries, theoretical tests using the method presented by Alcoverro and LePichon (2004) are required to determine the effect of one or more of the capillary plugs becoming partially or fully blocked by water, insects, etc. on the response of the individual filters and of the entire array. The long-term maintenance of these systems might involve periodic inspection and clearing of the capillary plugs.

Rosette spatial filters are used at almost all IMS infrasound arrays. All new filters include resonance-suppressing capillaries installed adjacent to the secondary summing manifolds, as described in this paper. Many of the existing filters are now being retro-fitted with capillaries. As a result, we anticipate an abundance of data in the near future will allow researchers to address these issues.

ACKNOWLEDGMENTS

The authors are indebted Chris Hayward (SMU) and Doug Christie (CTBTO) for suggesting that we experiment with capillaries. Frank Vernon, Jennifer Eakins, and Glen Offield provided the real-time data link. Clint Coon provided field assistance. Many helpful comments were provided by Lou Sutherland and two anonymous reviewers. Funding was provided by the Defense Threat Reduction Agency under Contract No. DTRA01-00-C-0085. Funding for the rosette filters used in this study was provided by the Defense Threat Reduction Agency (under Contract No. DTRA01-00-C-0085), the Provisional Technical Secretariat (PTS) of the UN

Comprehensive Test Ban Treaty Office in Vienna, and the US Army Space and Missile Defense Command (SMDC) University Research Initiative (URI).

Alcoverro, B. (1998). "Proposition d'un systeme de filtrage acoustique pour une station infrason IMS," CEA-DASE Scientific Report No. 241.
Alcoverro, B., and Le Pichon, A. (2004). "Design and optimization of a noise reduction system for Infrasound measurements using elements with low acoustic impedance," J. Acoust. Soc. Am.
Burrige, R. (1971). "The acoustics of pipe arrays," Geophys. J. R. Astron. Soc. **26**, 53–70.
Christie, D. R. (1999). "Wind-Noise-Reducing-Pipe Arrays," Report IMS-

IM-1999-1, Comprehensive Nuclear-Test-Ban Treaty Organization, Vienna Austria.
Christie, D. R., Vivas Veloso, J. A., Campus, P., Bell, M., Hoffmann, T., Langlois, A., Martysevich, P., Demirovich, E., and Carvalho, J. (2001). "Detection of atmospheric nuclear explosions: the infrasound component of the International Monitoring System," Kerntechnik **66**, 96–101.
Daniels, F. B. (1959). "Noise reducing line microphone for frequencies below 1 c/s," J. Acoust. Soc. Am. **31**, 529.
Donn, W. L., and Posmentier, E. S. (1967). "Exploring the Atmosphere with Nuclear Explosions," Rev. Geophys. **5**, 53.
Grover, F. H. (1971). "Experimental noise reducers for an active microbarograph array," J. Geophys. Soc. **26**, 41–52.
Hedlin, M. A. H., Alcoverro, B., and D'Spain, G. (2003). "Evaluation of rosette infrasonic noise-reducing spatial filters," J. Acoust. Soc. Am. **114**, 1807–1820.